Self-Diffusion Coefficients in Solutions of Lithium Bis(fluorosulfonyl)imide with Dimethyl Carbonate and Ethylene Carbonate

Johannes Neuhaus, Daniel Bellaire, Maximilian Kohns, Erik von Harbou*, and Hans Hasse

Dedicated to Prof. Dr. techn. Hans-Jörg Bart on the occasion of his 65th birthday

Organic solutions of lithium bis(fluorosulfonyl)imide (LiFSI) are promising electrolytes for Li-ion batteries. Information on the diffusion coefficients of the species in these solutions is needed for battery design. Therefore, the self-diffusion coefficients in such solutions were studied experimentally with the pulsed-field gradient nuclear magnetic resonance technique. The self-diffusion coefficients of the ions Li^+ and FSI^- as well as those of the solvents were measured for LiFSI solutions in pure dimethyl carbonate and ethylene carbonate as well as in mixtures of these solvents at 298 K and ambient pressure. Despite the Li^+ ion being the smallest species in the solution, its self-diffusion coefficient is the lowest as a result of its strong coordination with the solvent molecules.

Keywords: Diffusion, Electrolyte solutions, NMR spectroscopy

1 Introduction

Lithium-ion batteries (LiB) are widely used for storing electric energy [1, 2]. Advances in the field of electrolyte solutions can contribute to the progress of this technology [3–5]. Presently, the benchmark for LiB electrolytes is lithium hexafluorophosphate (LiPF6). Lithium bis(fluorosulfonyl)imide (LiFSI) is a promising candidate to replace LiPF6 [6–9]. Interesting solvents for LiFSI in LiB electrolytes are dimethyl carbonate (DMC) and ethylene carbonate (EC) [7, 8, 10]. Solutions of LiFSI in these solvents have a high electrical conductivity [6, 11–17].

Information on diffusion coefficients is of great interest for the modeling of transport processes in LiB and the rational design of LiB electrolyte solutions [14]. Despite the high interest in LiFSI-based electrolyte solutions, little is known to date on diffusion coefficients in LiFSI solutions in solvents such as DMC and EC. In the literature, there are only few reports on the diffusion coefficients of systems containing LiFSI. Takekawa et al. [18] report self-diffusion coefficients for a 1 M solution of LiFSI in the solvent mixture ethylene carbonate-diethyl carbonate (volume ratio 3/7). Tominga and Yamazaki [19] report self-diffusion coefficients for LiFSI solutions in poly(ethylene carbonate). Girard et al. [20] and Yoon et al. [21] report such data for LiFSI solutions in ionic liquids.

Therefore, in the present work, the pulsed field gradient nuclear magnetic resonance technique (PFG-NMR) was applied to determine the self-diffusion coefficients of the Li^+ and the FSI^- ions and that of the solvent molecules in LiFSI solutions in the pure solvents DMC and EC and mixtures of these solvents for LiFSI concentrations up to 0.2 mol mol^{-1} at 298 K and ambient pressure. Empirical correlations of the experimental data are provided.

2 Chemicals

Lithium bis(fluorosulfonyl)imide (LiFSI, $\geq$ 0.999 g g^{-1}) was supplied by Budan Process UG. Dimethyl carbonate (DMC, anhydrous, $\geq$ 0.999 g g^{-1}), and ethylene carbonate (EC, anhydrous, 0.990 g g^{-1}) were purchased from Sigma Aldrich. All chemicals were used as received. The water content of the pure components was determined by coulometric Karl-Fischer titration (Metrohm 831 KF coulometer) and was found to be below 50 · 10^{-6} g g^{-1} for all solvents and below 30 · 10^{-6} g g^{-1} for LiFSI. All chemicals were stored in an inert gas glove box (GS Glovebox Technik) that maintained a
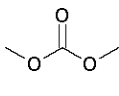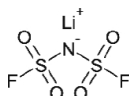
Dr. Johannes Neuhaus, Daniel Bellaire, Dr. Maximilian Kohns, Dr. Erik von Harbou, Prof. Dr.-Ing. Hans Hasse
erik.vonharbou@mv.uni-kl.de
University of Kaiserslautern, Laboratory of Engineering Thermodynamics (LTD), Erwin-Schrödinger Straße 44, 67663 Kaiserslautern, Germany.

nitrogen atmosphere with a water content of less than $2 \cdot 10^{-6}\,\mathrm{g\,g^{-1}}$.

Some relevant physico-chemical properties of the employed solvents and electrolytes are shown in Tab. 1, wherein M is the molar mass, T_nmp and T_nbp are the normal melting point and the normal boiling point, respectively, ρ is the density, η is the shear viscosity, D is the self-diffusion coefficient, and ε is the dielectric constant.

Table 1. Overview of some pure component physico-chemical properties. The numbers for ρ, η, D, and ε for DMC and EC refer to the liquid state at 313.15 K and ambient pressure.

Property	DMC	EC	LiFSI
	$C_3H_6O_3$	$C_3H_4O_3$	$F_2LiNO_4S_2$
M [g mol^{-1}]	90.1	88.1	187.1
T_nmp [K]	278.2 [22]	311.2 [22]	418.2 [6]
T_nbp [K]	363.15 [23]	517.15 [23]	
ρ [g cm^{-3}]	1.0434 [24]	1.3216 [25]	
η [mPa s]	0.4880 [26]	1.9000 [27]	
D [10^{-10} m^{2}s^{-1}]	26.0* [28]	8.0 [28]	
ε [–]	3.2 [29]	89.7 [30]	

*measured at 303.15 K

3 Experimental Method

3.1 Sample Preparation

All chemicals were handled in the inert gas glove box described above. A laboratory balance (Mettler-Toledo AG204) with an accuracy of ±0.0001 g according to the calibration protocol was used for the gravimetrical sample preparation. The total mass of each prepared sample was larger than 10 g. The samples were sealed in 20-mL glass vials. The uncertainty of the mole fraction of LiFSI and solvents is estimated to be ±0.0002 mol mol^{-1}.

3.2 PFG-NMR Measurements

^{1}H-, ^{7}Li-, and ^{19}F-NMR measurements were conducted using an NMR spectrometer with a superconducting magnet with a magnetic field strength of 9.4 T, corresponding to a proton Larmor frequency of 400.25 MHz. The NMR spectrometer was equipped with a probe with cryogenically cooled electronics (magnet Ascend 400, console Avance III HD 400, probe CryoProbe Prodigy, Bruker Biospin, Germany). The spectrometer's temperature sensor was calibrated with a platinum resistance thermometer (Pt-100) which in turn was calibrated in the laboratory using a certified standard. The stability of the thermostating gas flow is ±0.05 K. The overall uncertainty of the temperature measurement is estimated to be below ±0.15 K. Special NMR sample tubes with a capillary bottom with a bottom outer diameter of 2.5 mm (Deutero GmbH, Germany) were used in order to minimize the convection inside the sample and to reduce radiation damping. [31, 32]

The stimulated spin-echo technique with bipolar pulsed gradients [33] was applied as implemented in the spectrometer software (Bruker TopSpin 3.2, pulse sequence: stebpgp1s). The self-diffusion coefficient of species i (D_i) is obtained from a fit of the natural logarithm of the relative signal intensity against the squared gradient strength according to Eq. (1) [34]

$$\ln\left(\frac{I_i}{I_{0,i}}\right) = -D_i\gamma^2\delta^2\left(\Delta - \frac{1}{3}\delta\right)g^2 \tag{1}$$

where I_i and $I_{0,i}$ are the signal intensities of species i with and without gradient, respectively, γ is the gyromagnetic ratio, δ is the duration of the gradient pulse and g is the gradient strength. Δ is the diffusion time. The sum of the squared relative errors between the experimental data and the correlation was employed as the objective function in the fit.

The gradient strength g was obtained by the procedure proposed by Connell et al. [35] from experimental test measurements of water. The diffusion time Δ was chosen as 50 ms for all measurements and the gradient strength g was incremented following a square root relationship from 2.5 G cm^{-1} to 48.5 G cm^{-1}. Each diffusion experiment consisted of 16 transients with 16 scans, respectively, with a recycle delay that was chosen sufficiently long to ensure complete magnetization relaxation.

The gradient pulse duration δ was chosen in the range between 0.6 ms and 14 ms depending on the magnitude of the self-diffusion coefficients. Baseline and phase correction of the spectra were performed in the processing tool developed by Sawall et al. [36]. The relative standard uncertainty of the self-diffusion coefficients is estimated to be ±2 %. This is confirmed by test measurements on several well-studied systems that are not documented here.

4 Correlations

4.1 LiFSI in Pure DMC and EC

For correlating the experimental data for the self-diffusion coefficients in LiFSI solutions in the pure solvents DMC and EC, Eqs. (2) and (3) were applied.

$$\left(\frac{D_i}{\mathrm{m^2s^{-1}}}\right) = \left(\frac{D_{0,i}}{\mathrm{m^2s^{-1}}}\right) + A_i\left(\frac{x_\mathrm{LiFSI}}{\mathrm{mol\,mol^{-1}}}\right) + B_i\left(\frac{x_\mathrm{LiFSI}}{\mathrm{mol\,mol^{-1}}}\right)^2 \tag{2}$$

with i = (DMC, EC),

$$\left(\frac{D_j}{\mathrm{m^2s^{-1}}}\right) = \left(\frac{D_j^{x_i \to 1}}{\mathrm{m^2s^{-1}}}\right) + A_j\left(\frac{x_{\mathrm{LiFSI}}}{\mathrm{mol\,mol^{-1}}}\right) + B_j\left(\frac{x_{\mathrm{LiFSI}}}{\mathrm{mol\,mol^{-1}}}\right)^2 \tag{3}$$

with $j = (\mathrm{Li^+, FSI^-})$.

Here, x_{LiFSI} is the apparent mole fraction of LiFSI. D_i is the self-diffusion coefficient of the solvent $i = (\mathrm{DMC, EC})$ and D_j is that of ion $j = (\mathrm{Li^+, FSI^-})$. $D_{0,i}$ is the self-diffusion coefficient of the pure solvent i and $D_j^{x_i} \to 1$ is the self-diffusion coefficient of ion j at infinite dilution in solvent i. The parameters A_k, B_k ($k = i, j$), and $D_j^{x_i} \to 1$ are adjustable. In the case of EC also $D_{0,i}$ is used as an adjustable parameter, as pure EC is solid at 298 K and a self-diffusion coefficient for the liquid cannot be measured.

4.2 LiFSI in Binary Mixtures of DMC and EC

For correlating the experimental data for the self-diffusion coefficients in LiFSI solutions in binary mixtures of the solvents DMC and EC, the mixing rules shown in Eqs. (4) and (5) were used.

$$D_i = \tilde{x}_i D_i^{\tilde{x}_i \to 1} + (1 - \tilde{x}_i)D_i^{\tilde{x}_i \to 0} + \tilde{x}_i(1 - \tilde{x}_i)C_i \tag{4}$$

with $i = (\mathrm{DMC, EC})$,

$$D_j = \tilde{x}_i D_j^{\tilde{x}_i \to 1} + (1 - \tilde{x}_i)D_j^{\tilde{x}_i \to 0} + \tilde{x}_i(1 - \tilde{x}_i)C_j \tag{5}$$

with $j = (\mathrm{Li^+, FSI^-})$.

where $\tilde{x}_i$ is the mole fraction of solvent i in the salt-free solvent mixture. $D_i^{\tilde{x}_i \to 1}$ and $D_j^{\tilde{x}_i \to 1}$ are the self-diffusion coefficients of solvent i and ions j in LiFSI solutions in pure solvent i, respectively. $D_i^{\tilde{x}_i \to 0}$ and $D_j^{\tilde{x}_i \to 0}$ are the self-diffusion coefficients of solvent i and ion j in the other solvent, respectively. $D_i^{\tilde{x}_i \to 1}$, $D_j^{\tilde{x}_i \to 1}$, and $D_j^{\tilde{x}_i \to 0}$ in Eqs. (4) and (5) are calculated through Eqs. (2) and (3) for a given LiFSI concentration of x_{LiFSI} (here 0.10 mol mol^{-1}). $D_i^{\tilde{x}_i \to 0}$, C_i, and C_j are adjustable parameters.

4.3 Parameter Estimation

The adjustable parameters were determined from a fit to the corresponding experimental data. The sum of the squared relative deviations between the experimental data and the correlation was employed as objective function.

5 Results and Discussion

5.1 LiFSI in Pure DMC and EC

Fig. 1 shows the self-diffusion coefficients of all species in LiFSI solutions in DMC and EC, respectively, as a function

of the mole fraction of LiFSI at 298 K. The numerical experimental data are reported in Tab. 2, the correlation parameters in Tab. 3. The correlations describe the experimental data within the experimental uncertainty. An exception are the self-diffusion coefficients of the ions Li$^+$ and FSI$^-$ in LiFSI-DMC solutions for mole fractions of LiFSI below 0.05 mol mol^{-1}, which show higher deviations. The latter points were excluded from the fitting procedure but are shown for consistency. For LiFSI-EC solutions no self-diffusion coefficients could be determined below a mole fraction of LiFSI of 0.075 mol mol^{-1}, as a result of the low melting temperature of the mixture.
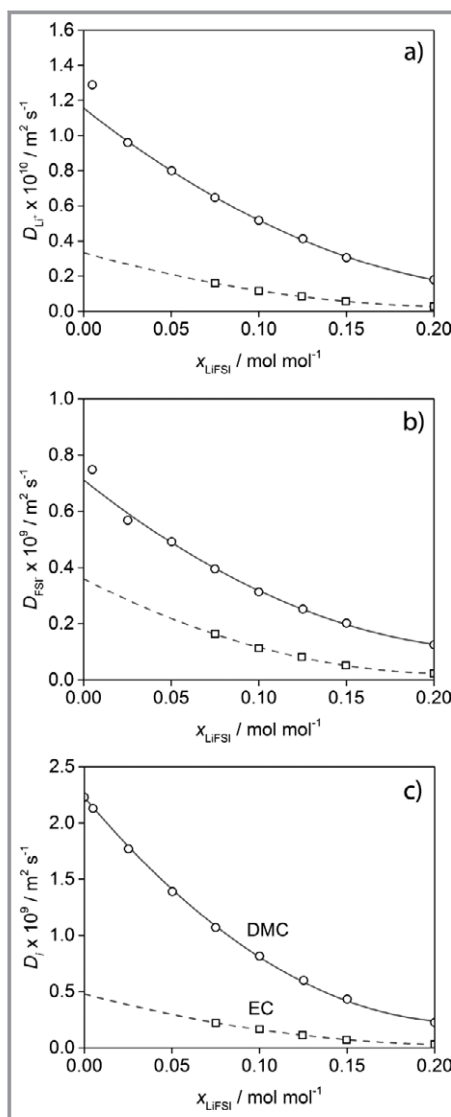

Figure 1. Self-diffusion coefficients of a) Li$^+$, b) FSI$^-$, and c) solvent molecules in LiFSI solutions in pure DMC and pure EC as a function of the mole fraction of LiFSI at 298 K. Symbols represent the experimental data for LiFSI solutions in pure DMC (circles) and pure EC (squares). Lines represent the correlations to these data using Eqs. (2) and (3) with parameters from Tab. 3.

Table 2. Experimental data for the self-diffusion coefficients in LiFSI solutions in pure DMC and pure EC at 298 K and ambient pressure.

LiFSI-DMC				LiFSI-EC			
x_{LiFSI} [mol mol^{-1}]	D_{Li^+} [10^{-11} m^{2}s^{-1}]	D_{FSI^-} [10^{-10} m^{2}s^{-1}]	D_{DMC} [10^{-9} m^{2}s^{-1}]	x_{LiFSI} [mol mol^{-1}]	D_{Li^+} [10^{-11} m^{2}s^{-1}]	D_{FSI^-} [10^{-10} m^{2}s^{-1}]	D_{EC} [10^{-10} m^{2}s^{-1}]
0.0000			2.23	0.0751	1.60	1.64	2.21
0.0050	12.90	7.49	2.13	0.1001	1.15	1.12	1.66
0.0252	9.61	5.68	1.77	0.1246	0.85	0.81	1.11
0.0503	8.00	4.91	1.39	0.1498	0.57	0.51	0.70
0.0750	6.47	3.95	1.07	0.2000	0.28	0.23	0.30
0.1000	5.17	3.13	0.82				
0.1252	4.13	2.52	0.60				
0.1501	3.06	2.02	0.43				
0.2000	1.78	1.25	0.23				

Standard uncertainties: $u(x) = 0.0002$ mol mol^{-1}, $u_r(D) = 0.02$.

Qualitatively, the self-diffusion coefficients in solutions of LiFSI in DMC and EC show the same behavior. Increasing the mole fraction of LiFSI results in a decrease of the self-diffusion coefficients of all species in all solutions. This goes along with a strong increase of the viscosity of the studied solutions.[11]

For a specific mole fraction of LiFSI, the self-diffusion coefficients of the ions Li$^+$ and FSI$^-$ are significantly lower for LiFSI-EC than they are in DMC. Furthermore, also the decrease of the self-diffusion coefficient with increasing salt concentration is more pronounced in DMC than in EC. For both solvents, the self-diffusion coefficients decrease in the order $D_{solv} > D_{FSI^-} > D_{Li^+}$. This order indicates that the small and densely charged Li$^+$ ions are strongly coordinated by the solvent molecules. This coordination results in large, slowly diffusing complexes. As a result, despite being much larger, the FSI$^-$ ion shows a higher self-diffusion coefficient than the Li$^+$ ion. This finding shows that the interaction of the FSI$^-$ ion with the solvents is much weaker than that of the Li$^+$ ion with the solvents.

While the data for the ion diffusion coefficients can be correlated easily for LiFSI concentrations above about 0.05 mol mol^{-1}, the few data points that were taken in more diluted solutions do not perfectly fit into this picture. This could indicate structural physical differences of the diffusion in this highly diluted regime as compared to more concentrated solutions. It was not in the scope of the present study to elaborate on this point, which would probably also call for further investigations, e.g., via molecular dynamics and quantum chemical simulations.

5.2 LiFSI in Binary Mixtures of DMC and EC

Fig. 2 shows the self-diffusion coefficients in solutions of LiFSI in binary mixtures of DMC and EC for a constant mole fraction of LiFSI of 0.1 mol mol^{-1} at 298 K and ambient pressure. The data are plotted as a function of the mole fraction of EC in the salt-free solvent mixture. The numerical experimental data are reported in Tab. 4, the correlation

Table 3. Parameters of the correlation functions of the self-diffusion coefficients of the solvents (Eq. (2)) and ions (Eq. (3)) in LiFSI solutions in pure DMC and pure EC at 298 K and ambient pressure.

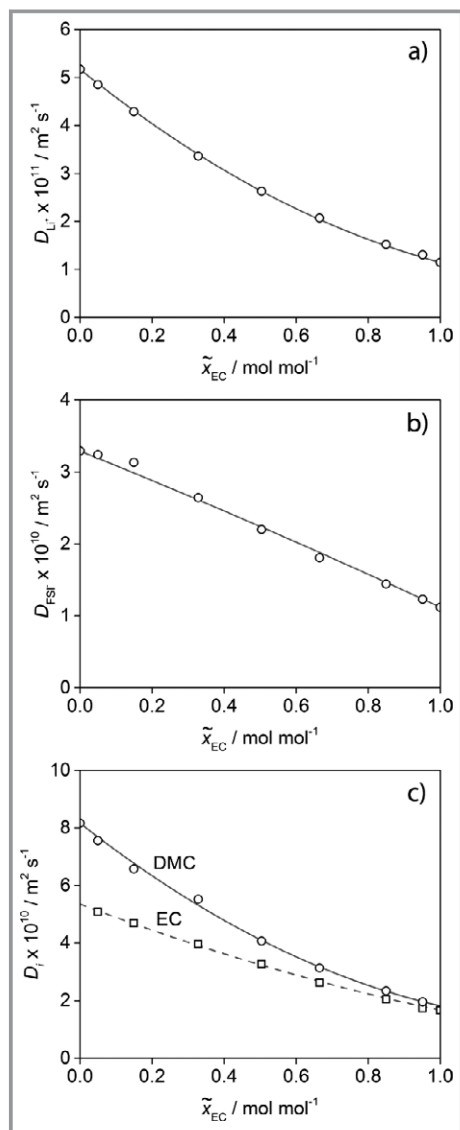| j	i	$D_{0,i}$	$D_j^{\bar{x}_i \to 1}$	A_i	A_j	B_i	B_j	R^2
	DMC	–	–	$-1.85 \cdot 10^{-8}$	–	$4.28 \cdot 10^{-8}$	–	0.9999
	EC	$4.80 \cdot 10^{-10}$	–	$-4.11 \cdot 10^{-9}$	–	$9.28 \cdot 10^{-9}$	–	0.9984
Li$^+$	DMC	–	$1.16 \cdot 10^{-10}$	–	$-7.86 \cdot 10^{-10}$	–	$1.49 \cdot 10^{-9}$	0.9993
Li$^+$	EC	–	$3.34 \cdot 10^{-11}$	–	$-2.80 \cdot 10^{-10}$	–	$6.37 \cdot 10^{-10}$	0.9993
FSI$^-$	DMC	–	$7.11 \cdot 10^{-10}$	–	$-4.94 \cdot 10^{-9}$	–	$1.01 \cdot 10^{-8}$	0.9999
FSI$^-$	EC	–	$3.60 \cdot 10^{-10}$	–	$-3.20 \cdot 10^{-9}$	–	$7.56 \cdot 10^{-9}$	0.9982

Figure 2. Self-diffusion coefficients of a) Li$^+$, b) FSI$^-$, and c) solvent molecules in solutions of LiFSI in binary mixtures of DMC and EC as a function of the mole fraction of EC in the salt-free solvent mixture at a mole fraction of LiFSI of 0.1 mol mol^{-1} at 298 K. Symbols represent the experimental data. Lines represent the correlations using Eqs. (4) and (5) with parameters from Tab. 5.

The self-diffusion coefficients of DMC and EC decrease with increasing salt-free mole fraction of EC. The self-diffusion coefficient of DMC at infinite dilution in EC is almost the same as the self-diffusion coefficient of pure EC. This finding can be attributed to the coordination complexes that have the form Li$^+$(EC)$_m$(DMC)$_n$ with $m + n = 4$. [37]

Due to their similar size, the Li$^+$(EC)$_3$(DMC)$_1$ complexes have virtually the same self-diffusion coefficient as the Li$^+$(EC)$_4$ complexes. In contrast to this, the self-diffusion coefficient of EC at infinite dilution in DMC is about 30 % lower than the self-diffusion coefficient of pure DMC. This observation shows that complexes comprising at least one EC molecule diffuse much slower than the Li$^+$(DMC)$_4$ complexes, as a result of their size.

6 Conclusions

In the present work, the self-diffusion coefficients of the Li$^+$ and FSI$^-$ ions and the solvent molecules in LiFSI solutions in the pure solvents DMC and EC as well as in mixtures of these solvents were investigated at 298 K. As expected, increasing the LiFSI concentration leads to a strong decrease of the self-diffusion coefficients of all species in all cases. The self-diffusion coefficients of the ions in DMC are higher than those in EC by a factor of about 3. The self-diffusion coefficient of Li$^+$ is about one order of magnitude lower than that of FSI$^-$ in all studied solvents, even though the FSI$^-$ ion is much larger than the Li$^+$ ion. This indicates a strong coordination of the Li$^+$ ions by the solvent molecules. The new data give quantitative information on the mobility of the species in the studied solutions, which are interesting electrolytes for LiB, and provide a basis for a better understanding of the transport processes in these systems.

parameters in Tab. 5. The experimental data for the diffusion coefficients of Li$^+$ and EC are described by the correlation within the uncertainty of the experimental data. For DMC and FSI$^-$, some deviations are observed. The self-diffusion coefficient of Li$^+$ depends significantly on the concentration of EC. From pure DMC to pure EC, it decreases by a factor of about 5.

Also, the self-diffusion coefficient of the FSI$^-$ ion decreases strongly upon addition of EC. From pure DMC to pure EC, it decreases by a factor of about 3. The simple correlation does not describe the experimental data perfectly. The slight S-shape of the data is not captured.

Table 4. Experimental data of the self-diffusion coefficients of DMC, EC, Li$^+$, and FSI$^-$ ion in LiFSI solutions in binary mixtures of DMC and EC for a mole fraction of LiFSI of 0.1 mol mol^{-1} at 298 K and ambient pressure.

$\tilde{x}_{EC}$ [mol mol^{-1}]	D_{Li^+} [10^{-11} m^{2}s^{-1}]	D_{FSI^-} [10^{-10} m^{2}s^{-1}]	D_{EC} [10^{-10} mm^{2}s^{-1}]	D_{DMC} [10^{-10} m^{2}s^{-1}]
0.0000	5.17	3.29		8.16
0.0494	4.85	3.24	5.09	7.56
0.1491	4.29	3.13	4.68	6.57
0.3282	3.36	2.64	3.96	5.52
0.5038	2.63	2.20	3.27	4.07
0.6650	2.07	1.81	2.62	3.13
0.8498	1.52	1.44	2.05	2.34
0.9513	1.30	1.23	1.73	1.96
1.0000	1.15	1.12	1.66	

Standard uncertainties: $u(x) = 0.0002$ mol mol^{-1}, $u_r(D) = 0.02$.

Table 5. Parameters of the correlation functions for the self-diffusion coefficients of the solvents i (Eq. (4)) and ions j (Eq. (5)) in LiFSI solutions in binary mixtures of DMC and EC for a mole fraction of LiFSI of 0.1 mol mol^{-1} at 298 K and ambient pressure. R^2 is the coefficient of determination.

	i		j	
	DMC	EC	Li$^+$	FSI$^-$
$D_i^{\tilde{x}_i \to 0}$	$1.82 \cdot 10^{-10}$	$5.36 \cdot 10^{-10}$		
C_k ($k = i, j$)	$-3.47 \cdot 10^{-10}$	$1.05 \cdot 10^{-10}$	$-2.05 \cdot 10^{-11}$	$-1.48 \cdot 10^{-11}$
R^2	0.9988	0.9970	0.9997	0.9950

References

[1] B. Scrosati, J. Garche, Lithium batteries: Status, prospects and future, *J. Power Sources* **2010**, *195*, 2419–2430.

[2] A. Thielmann, A. Sauer, M. Wietschel, *Gesamt-Roadmap Lithium-Ionen-Batterien 2030*, Fraunhofer-Institut für System- und Innovationsforschung ISI, Karlsruhe **2015**.

[3] S. S. Zhang, A review on electrolyte additives for lithium-ion batteries, *J. Power Sources* **2006**, *162*, 1379–1394.

[4] G. E. Blomgren, Electrolytes for advanced batteries, *J. Power Sources* **1999**, *81*, 112–118.

[5] G. E. Blomgren, The Development and Future of Lithium Ion Batteries, *J. Electrochem. Soc.* **2017**, *164*, A5019–A5025.

[6] H.-B. Han et al., Lithium bis(fluorosulfonyl)imide (LiFSI) as conducting salt for nonaqueous liquid electrolytes for lithium-ion batteries: Physicochemical and electrochemical properties, *J. Power Sources* **2011**, *196*, 3623–3632.

[7] W. Li, Use of lithium bis(fluorosulfonyl) imide (LiFSI) in non-aqueous electrolyte solutions for use with 4.2v and higher cathode materials for lithium ion batteries, *Patent WO2015073419A1*, **2017**.

[8] B. Hallac, M. C. Smart, F. C. Krause, B. M. Metz, R. V. Bugga, Lithium ion electrolytes with LiFSI for improved wide operating temperature range, *Patent US20160149263A1*, **2016**.

[9] L. Niedzicki, S. Grugeon, S. Laruelle, P. Judeinstein, M. Bukowska, J. Prejzner, P. Szczecinski, W. Wieczorek, M. Armand, New covalent salts of the 4+ V class for Li batteries, *J. Power Sources* **2011**, *196*, 8696–8700.

[10] M. S. Ding, T. R. Jow, K. Xu, Liquid-Solid Phase Diagrams of Binary Carbonates for Lithium Batteries, *J. Electrochem. Soc.* **2000**, *147*, 1688–1694.

[11] J. Neuhaus, E. von Harbou, H. Hasse, Physico-chemical properties of solutions of lithium bis(fluorosulfonyl)imide (LiFSI) in dimethyl carbonate, ethylene carbonate, and propylene carbonate, *J. Power Sources* **2018**, *394*, 148–159.

[12] S.-D. Han, O. Borodin, D. M. Seo, Z.-B. Zhou, W. A. Henderson, Electrolyte solvation and ionic association V. Acetonitrile-lithium bis (fluorosulfonyl) imide (LiFSI) mixtures, *J. Electrochem. Soc.* **2014**, *161*, A2042–A2053.

[13] S. Lux, I. Lucas, E. Pollak, S. Passerini, M. Winter, R. Kostecki, The mechanism of HF formation in LiPF6 based organic carbonate electrolytes, *Electrochem. Commun.* **2012**, *14*, 47–50.

[14] J. Neuhaus, E. Forte, E. von Harbou, H. Hasse, Electrical conductivity of solutions of lithium bis(fluorosulfonyl)imide in mixed organic solvents and multi-objective solvent optimization for lithium-ion batteries, *J. Power Sources* **2018**, *398*, 215–223.

[15] J. Wang, Y. Yamada, K. Sodeyama, C. H. Chiang, Y. Tateyama, A. Yamada, Superconcentrated electrolytes for a high-voltage lithium-ion battery, *Nat. Commun.* **2016**, *7*, 12032.

[16] L. Li, S. Zhou, H. Han, H. Li, J. Nie, M. Armand, Z. Zhou, X. Huang, Transport and Electrochemical Properties and Spectral Features of Non-Aqueous Electrolytes Containing LiFSI in Linear Carbonate Solvents, *J. Electrochem. Soc.* **2011**, *158*, A74–A82.

[17] S. Uchida, M. Ishikawa, Lithium bis(fluorosulfonyl)imide based low ethylene carbonate content electrolyte with unusual solvation state, *J. Power Sources* **2017**, *359*, 480–486.

[18] T. Takekawa, K. Kamiguchi, H. Imai, M. Hatano, Physicochemical and Electrochemical Properties of the Organic Solvent Electrolyte with Lithium Bis(fluorosulfonyl)Imide (LiFSI) As Lithium-Ion Conducting Salt for Lithium-Ion Batteries, *ECS Trans.* **2015**, *64*, 11–16.

[19] Y. Tominaga, K. Yamazaki, Fast Li-ion conduction in poly(ethylene carbonate)-based electrolytes and composites filled with TiO2 nanoparticles, *Chem. Commun.* **2014**, *50*, 4448–4450.

[20] G. M. A. Girard, M. Hilder, H. Zhu, D. Nucciarone, K. Whitbread, S. Zavorine, M. Moser, M. Forsyth, D. R. MacFarlane, P. C. Howlett, Electrochemical and physicochemical properties of small phosphonium cation ionic liquid electrolytes with high lithium salt content, *Phys. Chem. Chem. Phys.* **2015**, *17*, 8706–8713.

[21] H. Yoon, A. S. Best, M. Forsyth, D. R. MacFarlane, P. C. Howlett, Physical properties of high Li-ion content N -propyl-N-methyl-pyrrolidinium bis(fluorosulfonyl)imide based ionic liquid electrolytes, *Phys. Chem. Chem. Phys.* **2015**, *17*, 4656–4663.

[22] M. S. Ding, Liquid-Solid Phase Equilibria and Thermodynamic Modeling for Binary Organic Carbonates. *J. Chem. Eng. Data* **2004**, *49*, 276–282.

[23] O. Borodin, G. D. Smith, Quantum Chemistry and Molecular Dynamics Simulation Study of Dimethyl Carbonate: Ethylene Carbonate Electrolytes Doped with LiPF6, *J. Phys. Chem. B* **2009**, *113*, 1763–1776.

[24] R. Francesconi, F. Comelli, Vapor-Liquid Equilibria, Excess Molar Enthalpies, and Excess Molar Volumes of Dimethyl Carbonate + 1,2-Epoxybutane at 288.15, 298.15, or 313.15 K, *J. Chem. Eng. Data* **1996**, *41*, 736–740.

[25] P. T. Thompson, B. Fisher, R. H. Wood, Viscosities of solutions of electrolytes and non-electrolytes in ethylene carbonate at 40 °C, *J. Solution Chem.* **1982**, *11*, 1–15.

[26] A. Rodríguez, A. B. Pereiro, J. Canosa, J. Tojo, Dynamic viscosities of the ternary liquid mixtures (dimethyl carbonate + methanol + ethanol) and (dimethyl carbonate + methanol + hexane) at several temperatures, *J. Chem. Thermodyn.* **2006**, *38*, 505–519.

[27] S.-I. Tobishima, K. Hayashi, K.-I. Saito, J.-I. Yamaki, Ethylene carbonate-based ternary mixed solvent electrolytes for rechargeable lithium batteries, *Electrochim. Acta* **1995**, *40*, 537–544.

[28] K. Hayamizu, Y. Aihara, S. Arai, C. G. Martinez, Pulse-Gradient Spin-Echo 1H, 7Li, and 19F NMR Diffusion and Ionic Conductivity Measurements of 14 Organic Electrolytes Containing LiN(SO2CF3)2, *J. Phys. Chem. B* **1999**, *103*, 519–524.

[29] N. Nanbu, M. Takehara, S. Watanabe, M. Ue, Y. Sasaki, Polar Effect of Successive Fluorination of Dimethyl Carbonate on Physical Properties, *Bull. Chem. Soc. Jpn* **2007**, *80*, 1302–1306.

[30] R. Payne, I. E. Theodorou, Dielectric properties and relaxation in ethylene carbonate and propylene carbonate, *J. Phys. Chem.* **1972**, *76*, 2892–2900.

[31] K.-C. Chung, H.-Y. Yu, S.-D. Ahn, Convection Effects on PGSE-NMR Self-Diffusion Measurements at Low Temperature: Investigation into Sources of Induced Convective Flows, *Bull. Korean Chem. Soc.* **2011**, *32*, 1970–1974.

[32] V. Krishnan, N. Murali, Radiation damping in modern NMR experiments: Progress and challenges, *Prog. Nucl. Magn. Reson. Spectrosc.* **2013**, *68*, 41–57.

[33] D. H. Wu, A. Chen, C. S. Johnson, Flow Imaging by Means of 1D Pulsed-Field- Gradient NMR with Application to Electroosmotic Flow, *J. Magn. Reson.* **1995**, *115*, 123–126.

[34] E. O. Stejskal, J. E. Tanner, Spin Diffusion Measurements: Spin Echoes in the Presence of a Time-Dependent Field Gradient, *J. Chem. Phys.* **1965**, *42*, 288–292.

[35] M. A. Connell, P. J. Bowyer, P. A. Bone, A. L. Davis, A. G. Swanson, M. Nilsson, G. A. Morris, Improving the accuracy of pulsed field gradient NMR diffusion experiments: Correction for gradient non-uniformity, *J. Magn. Reson.* **2009**, *198*, 121–131.

[36] M. Sawall, E. von Harbou, A. Moog, R. Behrens, H. Schröder, J. Simoneau, E. Steimers, K. Neymeyr, Multi-objective optimization for an automated and simultaneous phase and baseline correction of NMR spectral data, *J. Magn. Reson.* **2018**, *289*, 132–141.

[37] O. Borodin, M. Olguin, P. Ganesh, P. R. C. Kent, J. L. Allen, W. A. Henderson, Competitive lithium solvation of linear and cyclic carbonates from quantum chemistry, *Phys. Chem. Chem. Phys.* **2016**, *18*, 164–175.